Hindawi
Mathematical Problems in Engineering
Volume 2022, Article ID 8461613, 9 pages
https://doi.org/10.1155/2022/8461613

Research Article

Chemically Reactive Flow and Energy Transport Phenomenon considering Variable Conductivity on Maxwell Fluid: A Numerical Simulation

Muavia Mansoor,[1] Yasir Nawaz,[2] Bilal Ahmad,[1] and Muhammad Irfan[3]

[1]*Department of Mathematics, University of Wah, Wah Cant, Pakistan*
[2]*Department of Mathematics, Air University, Islamabad, Pakistan*
[3]*Department of Mathematical Sciences, Federal Urdu University of Arts Science and Technology, Islamabad, Pakistan*

Correspondence should be addressed to Muhammad Irfan; mirfan@math.qau.edu.pk

Received 21 December 2021; Revised 6 April 2022; Accepted 20 April 2022; Published 19 May 2022

Academic Editor: A. M. Bastos Pereira

The present involvement is the theoretical use of the thermal extrusion structure accompanying with the various industrial progressions. The problem is composed by exploiting the MHD aspect on flow of Maxwell fluid. The properties of chemically reactive flow of magneto Maxwell fluid with effects of viscous dissipation over stretching sheet in stagnation region are elaborated here. The governing equations of phenomena are given in set of partial differential equations, and further these equations are reduced to set of ordinary differential equations using similarity transformations. MATLAB built in solver bvp4c is employed to solve obtained nonlinear boundary value problem. The solver uses the 4^{th} and 5^{th} order discretization scheme, and the outcomes in the form of velocity, temperature, and concentration profiles with variations of magnetic parameter, Maxwell parameter, heat generation parameter, Eckert number, Prandtl number, Schmidt number and reaction rate parameter are deliberated through graphs.

1. Introduction

During the last few decades, some of the researchers took great interest in the non-Newtonian fluid flow due to its practical applications. Their research accelerated due to the involvement of its applications in several chemical engineering processes, life sciences, and petroleum industries. Some important industrial fluids such as polymers, fossil fuels, pulps, food, and molten plastics show non-Newtonian fluids. The flow characteristics of both types of fluids (Newtonian and non-Newtonian) are explained in the form of constitutive equations. It is important to examine the flow behavior using these fluids and their several applications. A single equation is not capable of defining all the properties of non-Newtonian fluids and to overcome this deficiency, researchers have proposed different fluid models. The simplest models as discussed by researchers involve power law and grade fluid models. There is a major drawback of these simple models: the results obtained by these models are not compatible with flows. It is not able to guess the effects of elasticity. However, there is a special type of viscoelastic fluid called Maxwell fluid which explains the viscosity and elastic behavior of fluid which gains the attention of researchers. Aliakbar et al. [1] analyses its effect by considering the flow in applied magnetic fields with thermal radiation effects. Hayat and Qasim [2] extended their research by considering the same fluid with Joule heating effect. Shafiq and Khalique [3] examine upper convected Maxwell flow of stretching surface by using the Lie group methodology.

Stagnation point is the point during the fluid flow where the fluid velocity becomes zero. A conventional flow problem involved in the application of fluid mechanics is the two-dimensional flow near a stagnation point. Hiemenz [4] was the first to propose the work on stagnation point.

Homann [5] extended this work for an axisymmetric flow. Mahapatra and Gupta [6] investigated the effects of heat transfer during the stagnation point flow over the stretching surface, whereas its effects over shrinking sheet were analysed by Wang [7]. Mansur et al. [8] considered Buongiorno's model and analysed the effects of stagnation flow in nanofluids. Slip effects of the boundary layer flow near a stagnation point in the presence of magnetic field was discussed by Aman et al. [9]. Bachok and Ishak [10] considered the flow over nonlinearly stretching sheet and proposed a similarity solution for his model. Carbon nanotubes with single- and multiwalls influencing magnetohydrodynamic stagnation point nanofluid flow over variable thicker surfaces with concave and convex effects was studied by Shafiq et al. [11]. Considerable attention and a good amount of literature have been generated on this problem.

Viscous dissipation is a process in which the viscosity of fluid plays a significant role as it stores some amount of the kinetic energy of fluid particles during motion to its thermal energy and this process is an irreversible process. Brickman [12] primarily considered the effects of viscous dissipation. In his pioneer work, he considered the Newtonian fluid flow in a straight circular tube and proposed the result that the special effects were formed in the close region. Chand and Jat [13] considered the electrically conducting fluid and analysed thermal radiation effects together with viscous dissipation when the fluid is taken through a porous medium. Kishan and Deepa [14] considered the permeable sheet and drawn the numerical results of increasing the temperature of fluid due to the presence of viscous dissipation effects during the flow of micropolar fluid near the stagnation point. The effects of viscous dissipation and variable viscosity on moving vertical porous plate were reported by Singh [15]. Malik et al. [16] considered the Sisko fluid model for analyzing the effects contributed by viscous dissipation during the flow over a stretching cylinder. Shafiq et al. [17] studied the effects of viscous dissipation and Joule heating on Williamson fluid over stretching surface.

The major applications of the chemical reaction involved in chemical engineering processes are fibrous insulation, atmospheric flows, etc. Hayat et al. [18] discussed the impact on velocity and concentration of chemical species during the flow of upper [17] convective Maxwell fluid and used HAM to obtain the results of the proposed model. Bhattacharyya and Layek [19] reported the effects of chemical reaction by considering the electrically conducting fluid in a magnetic field over a vertical porous sheet and considered the same effects along with stagnation point in [20]. For more detail about this, see [21–23].

Keeping in view of the literature, the main aim of this study is to propose a model for the flow of Maxwell fluid over a stretching surface with combined effects of stagnation point and viscous dissipation in the presence of chemical species. The investigation will perform numerically with the help of computational software MATLAB. Possible flow patterns will also be drawn to visualize the flow behavior.

2. Problem Formulation

Consider the laminar incompressible, two-dimensional stagnation point flow of Maxwell fluid over a stretched plate. Let the plate be stretched with velocity $U_w = ax$ and $U_e = bx$ be the velocity at free stream. It is assumed that the x-axis$x$ – axis be taken along the plate and y-axis$y$ – axis be taken perpendicular to the plate and the motion of the flow is considered towards positive x-axis. x – axis. A magnetic field of constant strength B_0 is acting perpendicular to the plate. Let u and v be the horizontal and vertical components of velocity along x and y direction, respectively, T be temperature, and C be the concentration of the fluid. The geometry of this problem can be seen in Figure 1.

Under the boundary layer approximation and considering the effects of temperature-based thermal conductivity, viscous dissipation, heat generation, and chemical reaction, the governing Maxwell equations are expressed by [2, 3, 18]

$$\frac{\partial u}{\partial x} + \frac{\partial u}{\partial y} = 0, \tag{1}$$

$$u\frac{\partial u}{\partial x} + v\frac{\partial u}{\partial y} + \lambda_1\left(u^2\frac{\partial^2 u}{\partial x^2} + v^2\frac{\partial^2 u}{\partial y^2} + 2uv\frac{\partial^2 u}{\partial x\,\partial y}\right) = U_e\frac{dU_e}{dx} + v\frac{\partial^2 u}{\partial y^2} - \frac{\sigma {B_0}^2}{\rho}\left(u - U_e + \lambda_1 v\frac{\partial u}{\partial y}\right), \tag{2}$$

$$u\frac{\partial T}{\partial x} + v\frac{\partial T}{\partial y} = \frac{1}{\rho C_p}\frac{\partial}{\partial y}\left(k(T)\frac{\partial T}{\partial y}\right) + \frac{\mu}{\rho C_P}\left(\frac{\partial u}{\partial y}\right)^2 + \frac{Q_0}{\rho C_p}(T - T_\infty), \tag{3}$$

$$u\frac{\partial C}{\partial x} + v\frac{\partial C}{\partial y} = D\frac{\partial^2 C}{\partial y^2} - k_1(C - C_\infty). \tag{4}$$

Subject to the boundary conditions

$$\left.\begin{aligned} u = U_w, \quad v = 0,\ T = T_w,\ C = C_w \text{ at } y = 0 \\ u = U_e, \quad T = T_\infty,\ C = C_\infty \text{ at } y \longrightarrow \infty \end{aligned}\right\}, \tag{5}$$

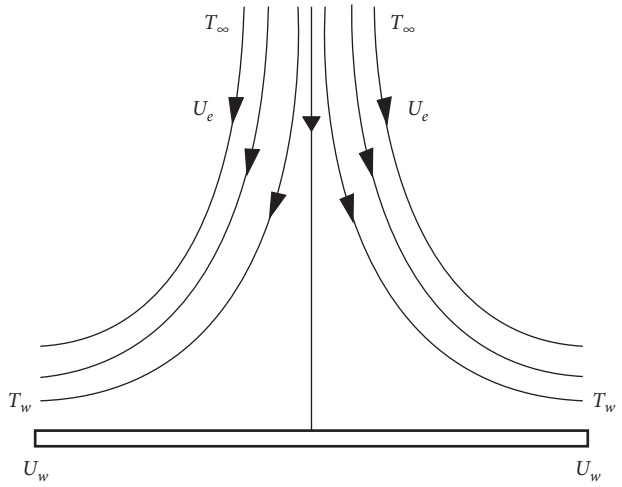

Figure 1: Geometry of the problem.

where $k(T) = k_\infty(1 - \epsilon\theta)$ is the variable conductivity, ν is the kinematic viscosity, σ is the electrical conductivity, λ_1 is the relaxation time, ρ is the fluid density, and k_1 is the reaction rate.

2.1. Transformation of the Governing System of Equations. By using nondimensional variables,

$$\eta = \sqrt{\frac{U_e}{\nu x}}y,$$

$$u = U_e f'(\eta),$$

$$v = -\sqrt{\frac{\nu U_e}{x}}f(\eta), \tag{6}$$

$$\theta = \frac{T - T_\infty}{T_w - T_\infty},$$

$$\varphi = \frac{C - C_\infty}{C_w - C_\infty}.$$

Continuity equation is identically satisfied, equations (2)–(4) can be written as follows:

$$f''' - \lambda f^2 f''' + f f'' + \lambda M^2 f f'' + 1 - f'^2 + M^2(1 - f') + 2\lambda f f' f'' = 0, \tag{7}$$

$$(1 - \epsilon\theta)\theta'' + pr\left(\delta\theta + Ec f''^2 + f\theta' - \frac{\theta'^2}{Pr}\right) = 0, \tag{8}$$

$$\varphi'' - Sc(\gamma\varphi - f\varphi\prime) = 0.$$

Subject to the boundary conditions,

$$\left.\begin{aligned} &f'(\eta) = \epsilon_1, \quad \theta(\eta) = 1, \ f(\eta) = 0, \ \varphi(\eta) = 1 \text{ at } \eta \longrightarrow 0 \\ &\theta(\eta) = 0, \quad f\prime(\eta) = 1, \ \varphi(\eta) = 0 \text{ at } \eta \longrightarrow \infty \end{aligned}\right\}, \tag{9}$$

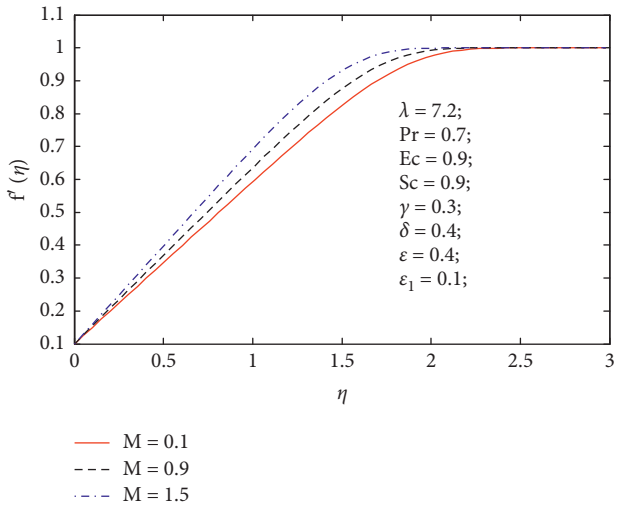

Figure 2: Velocity profile with variation of magnetic parameter M.

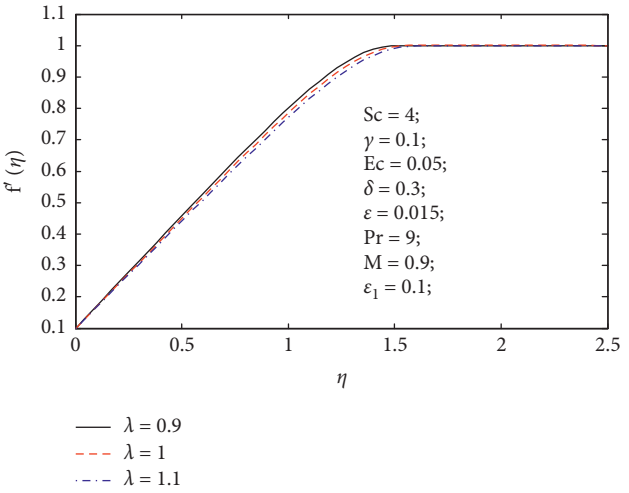

Figure 3: Velocity profile with variation of Maxwell parameterλ.

where $\lambda = a\lambda_1$ is the magnetic parameter, $M^2 = (\sigma B_0^2/\rho a)$ is the Maxwell parameter, $Pr = (C_p\mu_\infty/k_\infty)$ is the Prandtl number, $Sc = (\nu/D)$ is the Schmidt number, $\delta = (Q_0/a\rho C_p)$ is the heat absorption/generation parameter, $Ec = (U_e^2/C_p(T_w - T_\infty))$ is the Eckert number, and ϵ_1 is the ratio of stretching and free stream velocities.

3. Computational Procedure

Since the similarity method only gives the nondimensional equations which are further needed to be solved using some analytical or numerical method. In this section, the arise coupled nonlinear equations (2) to (4) together with boundary condition (5) are tackled numerically by MATLAB built in utility bvp4c. The MATLAB solver bvp4c solve scalar or system of differential equations using three-stage Lobatto IIIa formula. For giving the information of differential equations to the MATLAB solver, the conversion of the system of second- or higher-order differential equations into system of first-order ordinary differential equations is

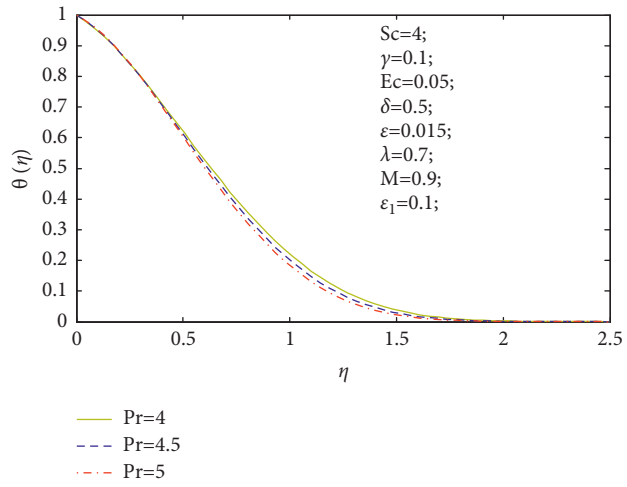

Figure 4: Temperature profile with variation of Prandtl numberPr.

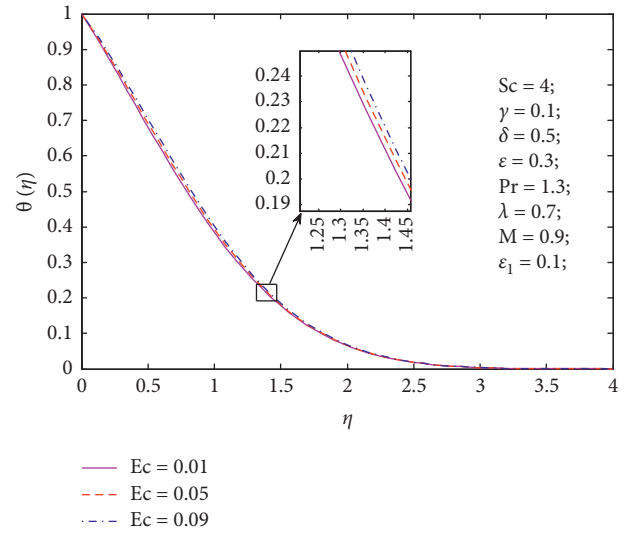

Figure 5: Temperature profile with variation of Eckert numberEc.

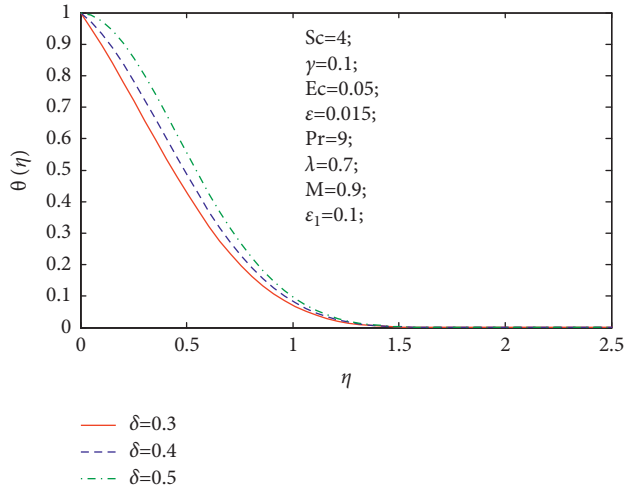

Figure 6: Temperature profile with variation of heat generation parameterδ.

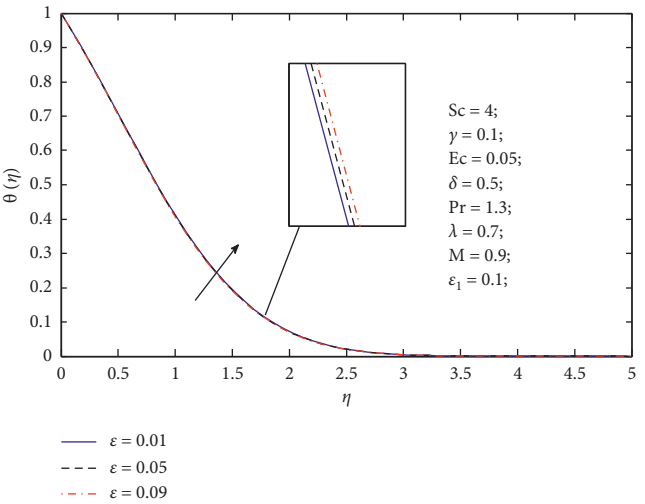

Figure 7: Temperature profile with variation of parameter ϵ.

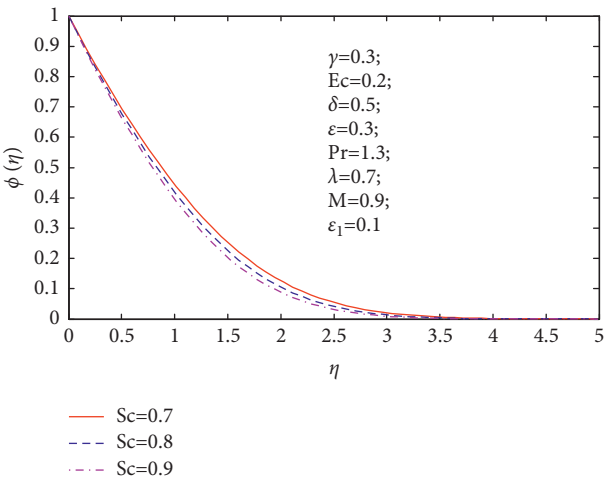

Figure 8: Concentration profile with variation of Schmidt number Sc.

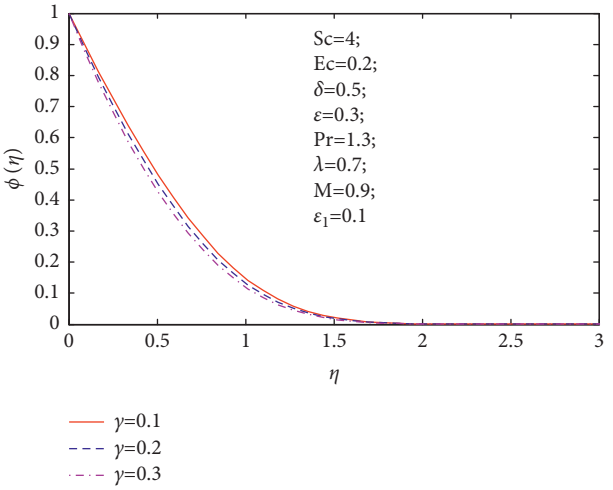

Figure 9: Concentration profile with variation of reaction rate parameter γ.

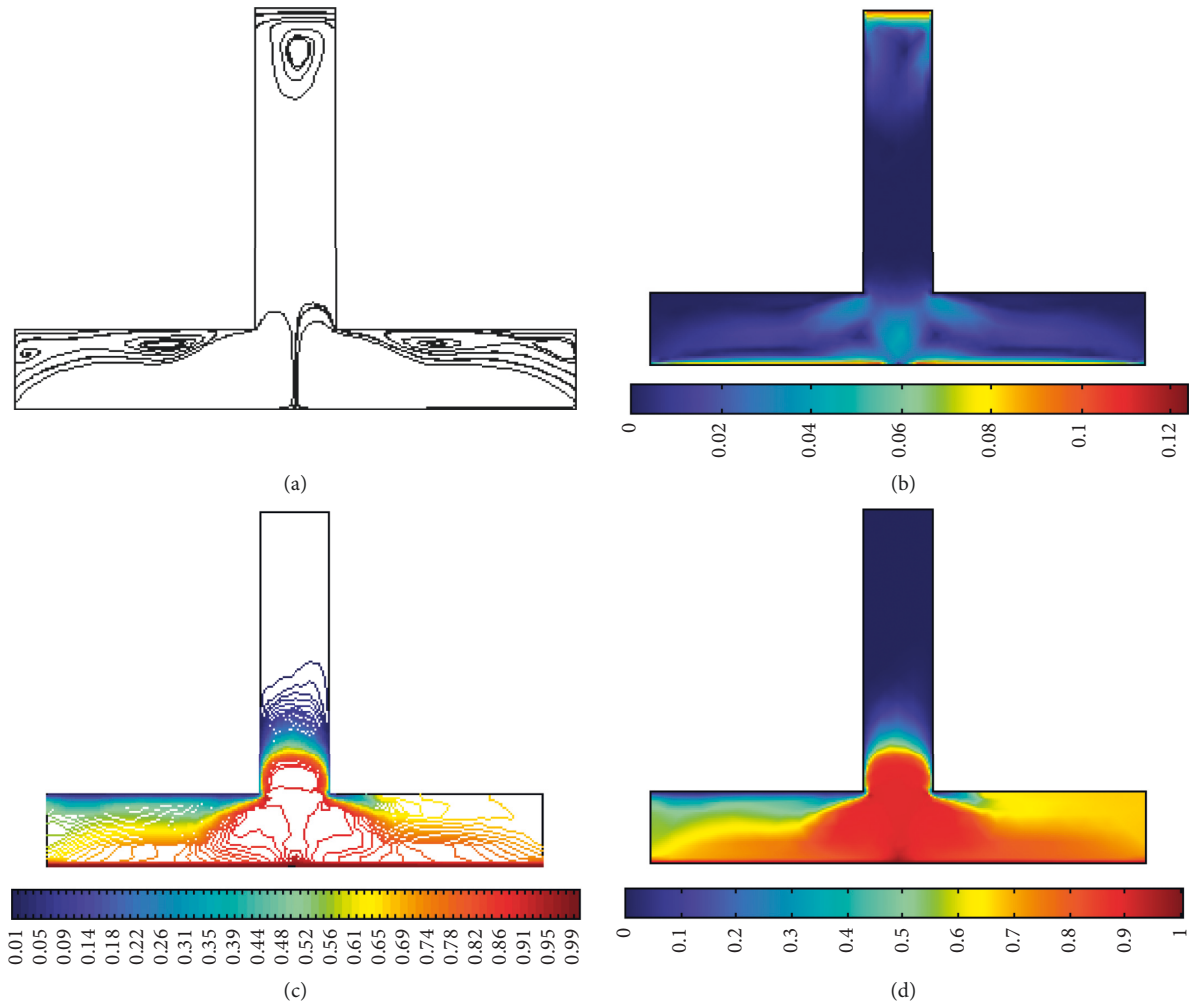

FIGURE 10: (a) Surface velocity plot. (b) Streamlines. (c) Temperature surface plot. (d) Isothermal contours using $U_e = 0.1$, $U_w = 0.1$ and $U_w = -0.1$ where $'+'\&'-'$ shows left and right translation respectively.

required. For this purpose, nonlinear equations are converted into first-order odes by invoking transformations in the following manners:

$$
\begin{aligned}
f' &= f_2,\\
f'' &= f_3,\\
f''' &= \frac{1}{\left(1-\lambda {f_1}^2\right)}\left(\left(1+\lambda M^2\right)f_1 f_3 + \left(1-f_2^2\right)\right.\\
&\quad \left. - M^2\left(f_2-1\right) + 2\lambda f_1 f_2 f_3\right),\\
\theta' &= f_5,\\
\theta'' &= \left(-\frac{pr}{a\left(1-\epsilon f_4\right)}\right)\left(\delta f_4 + Ec f_3^2 + a f_1 f_5 - \frac{a f_5^2}{Pr}\right),\\
\varphi' &= f_7,\\
\varphi'' &= Sc\left(\gamma f_6 - f f_7\right),
\end{aligned}
\tag{10}
$$

where $f = f_1$, $\theta = f_4$, and $\varphi = f_6$, and the boundary conditions can be specified by

$$
\left[f_{0,1}, f_{0,2} - \epsilon_1, f_{\text{inf},2} - 1, f_{0,4} - 1, f_{\text{inf},4}, f_{0,6} - 1, f_{\text{inf},6}\right]^t, \tag{11}
$$

where f_0 is used to describe the boundary condition for the left end point of the domain and f_{inf} is used to describe boundary conditions on the right end point of the domain for the equations (6)–(8) with boundary conditions (9).

4. Results and Discussions

The dimensionless sets of nonlinear ordinary differential equations have been solved by MATLAB solver bvp4c. This solver uses fourth and fifth order numerical method to solve given differential equations. It requires one set of initial guesses, to start the solving procedure. The set of first-order differential equations and set of boundary conditions are two of its inputs and the result can be seen through graphs. A one-dimension mesh may depend upon the user to choose grid points. Also, the mesh for initial conditions can be different from the mesh of the obtained solution.

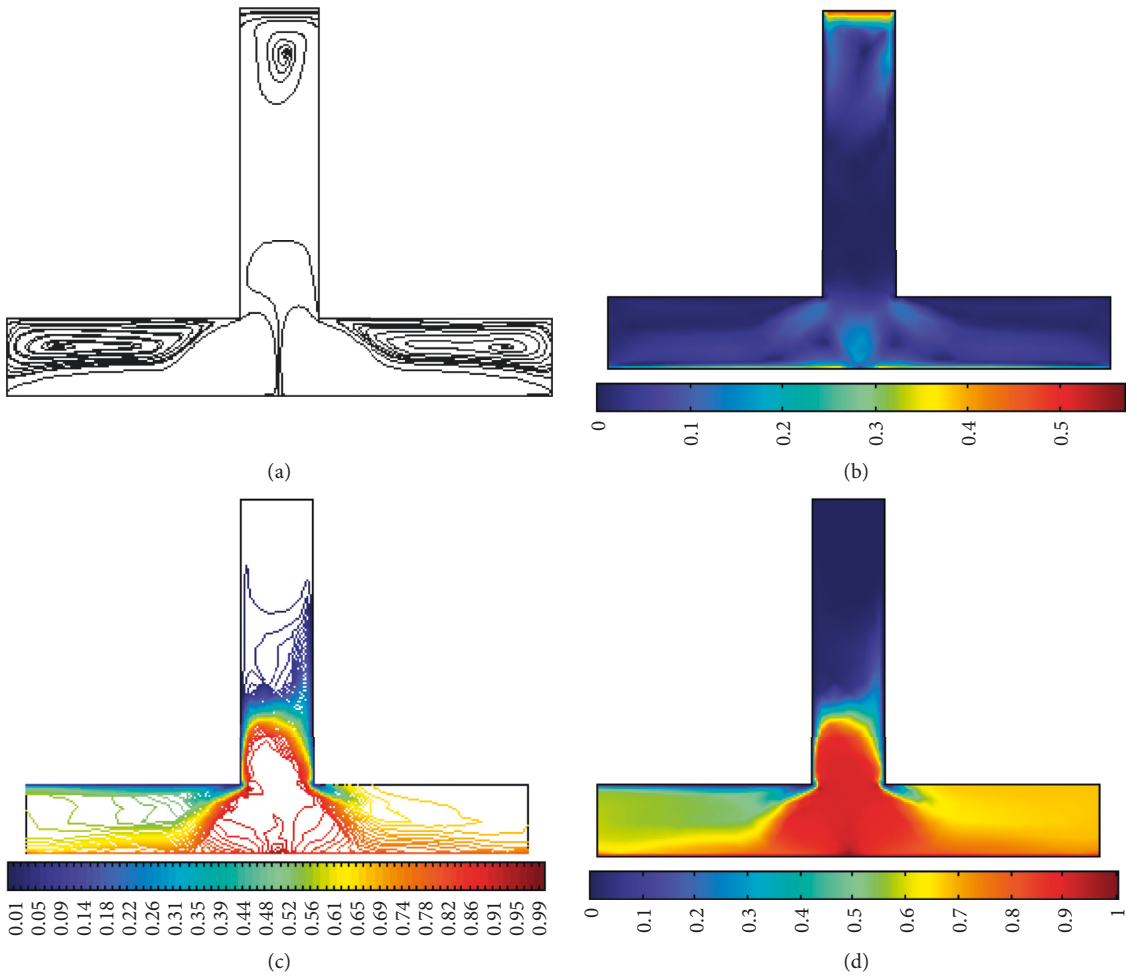

Figure 11: (a) Surface velocity plot (b) streamlines (c) temperature surface plot (d) Isothermal contours using $U_e = 0.5$, $U_w = 0.5$, and $U_w = -0.5$ where '+' and '−' shows left and right translation, respectively.

Figure 2 elucidates the impact of the magnetic parameter on velocity profile. The momentum boundary layer thickness decays by upraising the values of the magnetic parameter due to generation of the Lorentz force which is responsible for providing resistance to the velocity. Figure 3 elucidates the impact of Maxwell parameter on the velocity profile. The velocity de-escalates by raising the Maxwell parameter.

Figure 4 shows the impact of Prandtl number on temperature profile. The temperature de-escalates by enhancing the values of the Prandtl number. This happens due to decay of thermal diffusivity, and this decay is responsible for de-escalation of thermal conductivity and therefore the temperature of the fluid decreases. Figure 5 elucidates the impact of Eckert number on temperature profile. By looking at this Figure 5, it can be observed that the temperature is enhanced by upraising the values of the Eckert number. Figure 6 deliberates the impact of heat generation parameter on temperature profile. Temperature of the fluid escalates by enhancing the values of the heat generation parameter and this is happening due to an attached heat source that produces heat to the fluid and so the temperature of the fluid escalates. Figure 7 shows the impact of parameter ϵ on the temperature profile. By looking at Figure 7, it seems that the temperature enhanced by upraising the values of parameter ϵ. Physically, it describes the temperature gradients inside the material at the time of progress in addition to inside the materials. When ϵ increase, the magnitude of temperature also increases, which enhances the temperature field.

Figure 8 elucidates the behavior of concentration profile when Schmidt number varies. Figure 8 shows concentration decays by increasing the values of Schmidt number. The decrease of concentration is the consequence of using Fick's law because increasing values of the Schmidt number leads to slow down molecular flux and consequently molecular diffusion process becomes slow and so the concentration de-escalates. Figure 9 elucidates the impact of reaction rate parameter on concentration profile. From Figure 9, it can be observed that concentration decreases by upraising the values of reaction rate parameter.

Figures 10–12 are drawn using software which uses the finite element method to solve the partial differential equations. In these figures, variations of wall's velocity and free stream velocity are considered and found that the velocity of the fluid near to the plate is escalating by

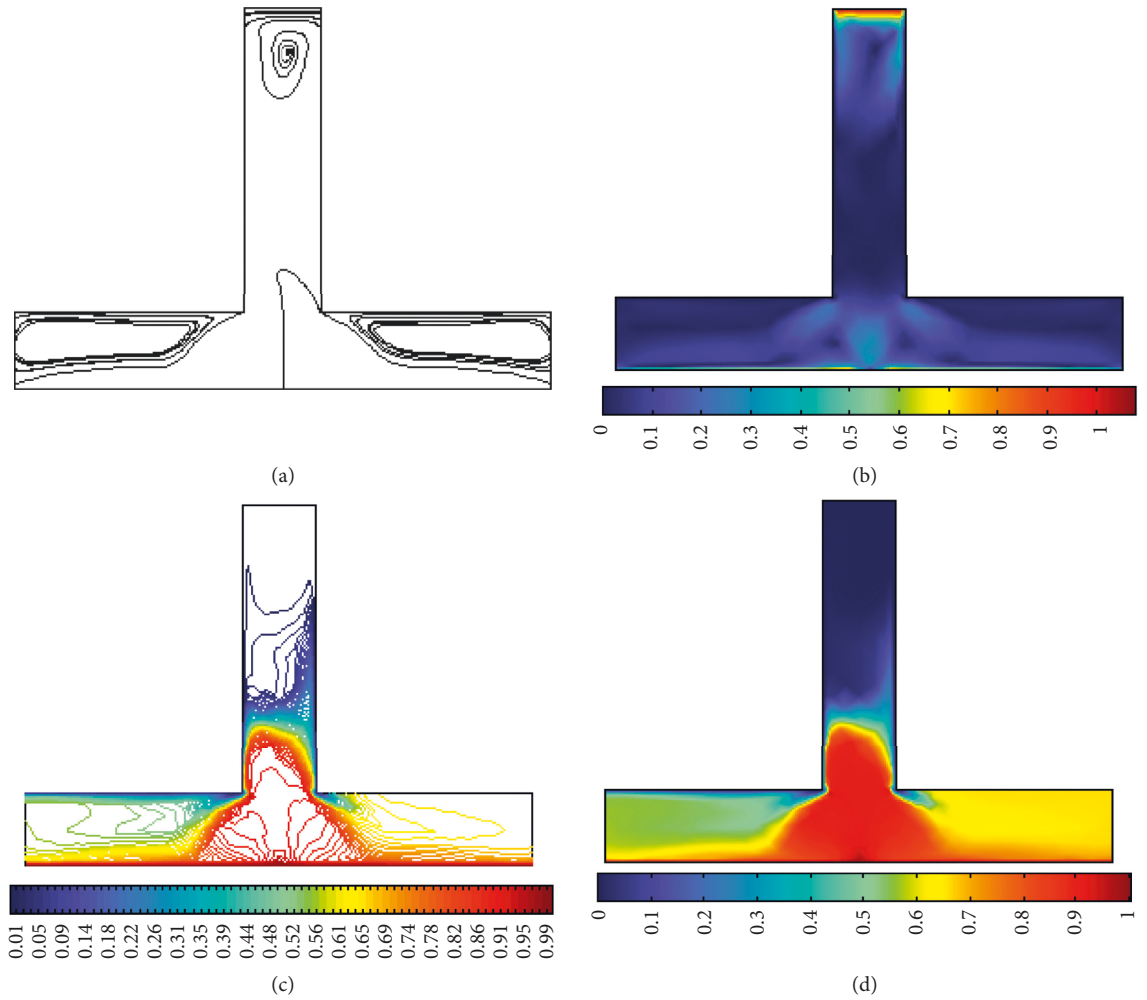

Figure 12: (a) Surface velocity plot. (b) Streamlines. (c) Temperature surface plot. (d) Isothermal contours using $U_e = 1$, $U_w = 1$, and $U_w = -1$ where $'+'$ and $'-'$ shows left and right translation, respectively.

Table 1: Numerical values of local Nusselt number and local Sherwood number with variation of parameters using $\epsilon_1 = 0.1$.

M	λ	Pr	Ec	Sc	γ	δ	ϵ	$-\theta'(0)$	$-\phi'(0)$
0.4	07	0.5	0.7	0.7	0.1	0.1	0.2	0.6118	0.5381
0.5	07	0.5	0.7	0.7	0.1	0.1	0.2	0.6113	0.5390
0.5	7.1	0.5	0.7	0.7	0.1	0.1	0.2	0.6113	0.5389
0.5	7.2	0.5	0.7	0.7	0.1	0.1	0.2	0.6114	0.5388
0.5	7.2	0.6	0.7	0.7	0.1	0.1	0.2	0.6080	0.5388
0.5	7.2	0.7	0.7	0.7	0.1	0.1	0.2	0.6045	0.5388
0.5	7.2	0.7	0.8	0.7	0.1	0.1	0.2	0.5722	0.5388
0.5	7.2	0.7	0.9	0.7	0.1	0.1	0.2	0.5404	0.5388
0.5	7.2	0.7	0.9	0.8	0.1	0.1	0.2	0.5404	0.5635
0.5	7.2	0.7	0.9	0.9	0.1	0.1	0.2	0.5404	0.5872
0.5	7.2	0.7	0.9	0.9	0.2	0.1	0.2	0.5404	0.6467
0.5	7.2	0.7	0.9	0.9	0.3	0.1	0.2	0.5404	0.7030
0.5	7.2	0.7	0.9	0.9	0.3	0.3	0.2	0.3663	0.7030
0.5	7.2	0.7	0.9	0.9	0.3	0.4	0.2	0.2725	0.7030
0.5	7.2	0.7	0.9	0.9	0.3	0.4	0.3	0.2581	0.7030
0.5	7.2	0.7	0.9	0.9	0.3	0.4	0.4	0.2351	0.7030

enhancing the velocity of wall and free stream velocity. The temperature also rises by upraising the velocity of wall and free stream velocity when varying the values from to 0.1 to 0.5, whereas the surface of temperature is approximately unchanged by increasing wall and free stream velocities from to 0.5 to 0.1.

Table 2: Comparison of the value of $-\theta'(0)$ for $M = \epsilon = \delta = \lambda = 0$ and $Ec = 0.3$.

Pr	[24]	[25]	Present
0.5	0.175815	0.176182	0.175812
1	0.299876	0.299877	0.299821
3	0.634113	0.634110	0.634119
5	0.870431	0.870427	0.870418
10	0.308613	0.308608	0.308631

Table 1 shows the numerical values for local Nusselt and local Sherwood numbers. From Table 1, it seems to be that the local Sherwood number escalates and de-escalates by growing values of magnetic parameter and Maxwell parameter, respectively. Local Nusselt number decays by the growth of the Prandtl number and Eckert number. Local Sherwood number increases by the rising Schmidt number. For validation and accuracy of our computations, Table 2 is presented in a limiting manner. Good agreement is achieved with the existing results.

5. Conclusion

The current study was comprised of mathematical model for two-dimensional, laminar, stagnation point flow of steady incompressible fluid with temperature-based thermal conductivity. This mathematical model was modified by using the similarity method and further governing system of equations are converted to set of ordinary differential equations (ODEs). MATLAB built in solver bvp4c has been implemented to solve set of ordinary differential equations. The major findings of this study are as follows:

(i) Velocity profile of the fluid was de-escalated by choosing larger values of the magnetic parameter.

(ii) Temperature profile was de-escalated by upraising the values of Prandtl number.

(iii) Concentration profile was decreased by upraising the values of Schmidt numbers.

Data Availability

There are no data available for this study.

Conflicts of Interest

The authors declare that they do not have any conflicts of interest.

References

[1] V. Aliakbar, A. Alizadeh-Pahlavan, and K. Sadeghy, "The influence of thermal radiation on MHD flow of Maxwellian fluids above stretching sheets," *Communications in Nonlinear Science and Numerical Simulation*, vol. 14, no. 3, pp. 779–794, 2009.

[2] T. Hayat and M. Qasim, "Influence of thermal radiation and Joule heating on MHD flow of a Maxwell fluid in the presence of thermophoresis," *International Journal of Heat and Mass Transfer*, vol. 53, no. 21-22, pp. 4780–4788, 2010.

[3] A. Shafiq and C. M. Khalique, "Lie group analysis of upper convected Maxwell fluid flow along stretching surface," *Alexandria Engineering Journal*, vol. 59, no. 4, pp. 2533–2541, 2020.

[4] K. Hiemenz, "Die Grenzschicht an einem in den gleichformigen Flussigkeitsstrom eingetauchten geraden Kreiszylinder," *Dinglers Polytech. J.*vol. 326, pp. 321–324, 1911.

[5] F. Homann, "Der Einfluß großer Zähigkeit bei der Strömung um den Zylinder und um die Kugel," *ZAMM - Zeitschrift für Angewandte Mathematik und Mechanik*, vol. 16, no. 3, pp. 153–164, 1936.

[6] T. R. Mahapatra and A. S. Gupta, "Heat transfer in stagnation-point flow towards a stretching sheet," *Heat and Mass Transfer*, vol. 38, no. 6, pp. 517–521, 2002.

[7] C. Y. Wang, "Stagnation flow towards a shrinking sheet," *International Journal of Non-linear Mechanics*, vol. 43, no. 5, pp. 377–382, 2008.

[8] S. Mansur, A. Ishak, and I. Pop, "Stagnation-point flow towards a stretching/shrinking sheet in a nanofluid using Buongiorno's model," *Proceedings of the Institution of Mechanical Engineers - Part E: Journal of Process Mechanical Engineering*, vol. 231, no. 2, pp. 172–180, 2017.

[9] F. Aman, A. Ishak, and I. Pop, "Magnetohydrodynamic stagnation-point flow towards a stretching/shrinking sheet with slip effects," *International Communications in Heat and Mass Transfer*, vol. 47, pp. 68–72, 2013.

[10] N. Bachok and A. Ishak, "Similarity solutions for the stagnation-point flow and heat transfer over a nonlinearly stretching/shrinking sheet," *Sains Malaysiana*, vol. 40, pp. 1297–1300, 2011.

[11] A. Shafiq, I. Khan, G. Rasool, E.-S. M. Sherif, and A. H. Sheikh, "Influence of single- and multi-wall carbon nanotubes on magnetohydrodynamic stagnation point nanofluid flow over variable thicker surface with concave and convex effects," *Mathematics*, vol. 8, no. 1, p. 104, 2020.

[12] H. C. Brinkman, "Heat effects in capillary flow I," *Applied Scientific Research*, vol. 2, no. 1, pp. 120–124, 1951.

[13] G. Chand and R. Jat, "Viscous dissipation and radiation effects on MHD flow and heat transfer over an unsteady stretching surface in a porous medium," *Thermal Energy and Power Engineering*, vol. 3, pp. 266–272, 2014.

[14] N. Kishan and G. Deepa, "Viscous dissipation effects on stagnation point flow and heat transfer of a micropolar fluid with uniform suction or blowing," *Advances in Applied Science Research*, vol. 3, pp. 430–439, 2012.

[15] P. Singh, "Viscous dissipation and variable viscosity effects on MHD boundary layer flow in porous medium past a moving vertical plate with suction," *International Journal of Engineering Science and Technology*, vol. 4, pp. 2647–2656, 2012.

[16] M. Y. Malik, A. Hussain, T. Salahuddin, and M. Awais, "Effects of viscous dissipation on MHD boundary layer flow of Sisko fluid over a stretching cylinder," *AIP Advances*, vol. 6, no. 3, Article ID 035009, 2016.

[17] A. Shafiq, M. M. Rashidi, Z. Hammouch, and I. Khan, "Analytical investigation of stagnation point flow of Williamson liquid with melting phenomenon," *Physica Scripta*, vol. 94, no. 3, Article ID 035204, 2019.

[18] T. Hayat, Z. Abbas, and N. Ali, "MHD flow and mass transfer of a upper-convected Maxwell fluid past a porous shrinking sheet with chemical reaction species," *Physics Letters A*, vol. 372, no. 26, pp. 4698–4704, 2008.

[19] K. Bhattacharyya and G. C. Layek, "Slip effect on diffusion of chemically reactive species in boundary layer flow over a vertical stretching sheet with suction or blowing," *Chemical*

Engineering Communications, vol. 198, no. 11, pp. 1354–1365, 2011.

[20] K. Bhattacharyya, S. Mukhopadhyay, and G. C. Layek, "Reactive solute transfer in magnetohydrodynamic boundary layer stagnation-point flow over a stretching sheet with suction/blowing," *Chemical Engineering Communications*, vol. 199, no. 3, pp. 368–383, 2012.

[21] T. Hayat, S. Qayyum, A. Alsaedi, and A. Shafiq, "Inclined magnetic field and heat source/sink aspects in flow of nanofluid with nonlinear thermal radiation," *International Journal of Heat and Mass Transfer*, vol. 103, pp. 99–107, 2016.

[22] A. Shafiq and T. N. Sindhu, "Statistical study of hydromagnetic boundary layer flow of Williamson fluid regarding a radiative surface," *Results in Physics*, vol. 7, pp. 3059–3067, 2017.

[23] T. N. Sindhu and A. Atangana, "Reliability analysis incorporating exponentiated inverse Weibull distribution and inverse power law," *Quality and Reliability Engineering International*, vol. 37, no. 6, pp. 2399–2422, 2021.

[24] E. Magyari and B. Keller, "Heat and mass transfer in the boundary layers on an exponentially stretching continuous surface," *Journal of Physics D: Applied Physics*, vol. 32, no. 5, pp. 577–585, 1999.

[25] M. Abd El-Aziz, "Viscous dissipation effect on mixed convection flow of a micropolar fluid over an exponentially stretching sheet," *Canadian Journal of Physics*, vol. 87, no. 4, pp. 359–368, 2009.